Acoustic-electric non-destructive method to detect defects in dielectric materials

A Bespal'ko, A Surzhikov, D Dann, E Pomishin, M Petrov

Tomsk Polytechnic University, Russia, Tomsk

besko48@tpu.ru

Abstract. The paper reveals the effect of imperfection of solid-state dielectric samples on the parameters of the electromagnetic response under exposure of the test object to deterministic acoustic impact. The patterns of changes in the parameters of electromagnetic signals with variations and an increased electric field vector with respect to the defect–sample contact are provided. It is shown that the amplitude-frequency parameters of the emitted electromagnetic signals are directly related to the acoustic impedance and conductivity of the contacting medium and defect. The amplitudes of the electromagnetic responses are found to correspond to the distribution of mechanical stresses arising in an imperfect system during acoustic pulse propagation in time and space determined through mathematical modeling. The paper presents data on changes in the electromagnetic signal parameters for model defects of an increased size in samples of similar type.

1. Introduction

A number of methods are currently used in non-destructive testing to detect defects in materials and products: acoustic, electrical and electromagnetic, magnetic, X-ray and others [1–8]. However, for dielectric materials and structures, this variety of non-destructive methods cannot be effectively used in all cases. This is due to high permeability of X-ray radiation, the absence of magnetic properties in the vast majority of dielectrics, and the close ratio of the acoustic impedance during ultrasonic sounding.

Early detection of imperfection of dielectric structures is of great importance for testing their mechanical and electrical strength. For safety reasons, insulators, structural organic dielectrics, concrete structures and other dielectric structures and products should be periodically subjected to non-destructive testing. In this regard, it is advisable to employ complex methods of non-destructive testing. This complex method can imply contact acoustic sounding of the test object and non-contact recording of the electromagnetic response to the impact followed by an amplitude-frequency analysis of the electromagnetic signal (EMS). The electromagnetic signal arises when electrical double layers on the edges of cracks and cavities start to vibrate and when the contact areas of materials, layers and other defects are polarized [9–18]. Mathematical modeling and laboratory studies have shown that these transformations are some of the main techniques to generate EMS in heterogeneous dielectric materials. Acoustic pulses propagate and interact with existing and newly emerging defects. As a result, charges or electrical double layers at the interfaces between media, inclusions or blocks, on edges of cracks or on other structural defects of dielectric materials emit electromagnetic signals.

In [19], theoretical studies provide physical demonstration of the electromagnetic method for testing heterogeneous dielectric materials. It is indicated that inducing mechanical vibrations by normalized single impact causes a bias current. The bias current in turn depends on the rate of the change in the bulk density of elementary sources and on the dipole moment. For the test samples, the magnitude of the surface charges, their spatial structure and amplitude of vibrations depend on physicochemical properties of the sample internal regions.

In [18–21], experimental studies show that the passage of acoustic waves causes EMS generation, which is associated with vibrations of the electrical double layers. It is revealed that acoustic-electrical transformations cause the transfer of the acoustic signal energy to the EMS energy. In this case, the EMS amplitude-frequency parameters depend on the parameters of acoustic pulses and the charge state of the existing defects in the form of inclusions and layered texture.

Thus, external deterministic acoustic impact and the parameters of electromagnetic responses to this disturbance can be used to successfully test dielectric materials to detect defects in the form of solid-state inclusions or voids. Numerical and experimental modeling of this testing was performed. This paper presents the findings of the experimental studies of changes in EMS parameters and spectra upon deterministic acoustic pulse excitation of model samples with defects in the form of solid-state inclusions.

2. Research methods

To study the effect of defects on the parameters of electromagnetic signals under deterministic acoustic pulse excitation, samples $(5.0\times5.0\times9.5)\times10^{-6}$ m^3 in size with defects inside were made of cement-sand mixture (CSM). The longitudinal acoustic pulse propagation velocity along the CSM sample was 2765 m/s, and the mixture density was 1900 kg/m^3. Rectangles with sizes of $(25\times25\times38)\times10^{-9}$ m^3, $(20\times20\times30)\times10^{-9}$ m^3, $(15\times15\times20)\times10^{-9}$ m^3, and $(10\times10\times15)\times10^{-9}$ m^3 made of plexiglass, fluoroplastic, ebonite, magnetite ore, limestone, brass, duralumin, and steel were used as defects. The position of the defect in the sample was verified by digital radiography using a PerkinElmer XRD 0822 detector [22].

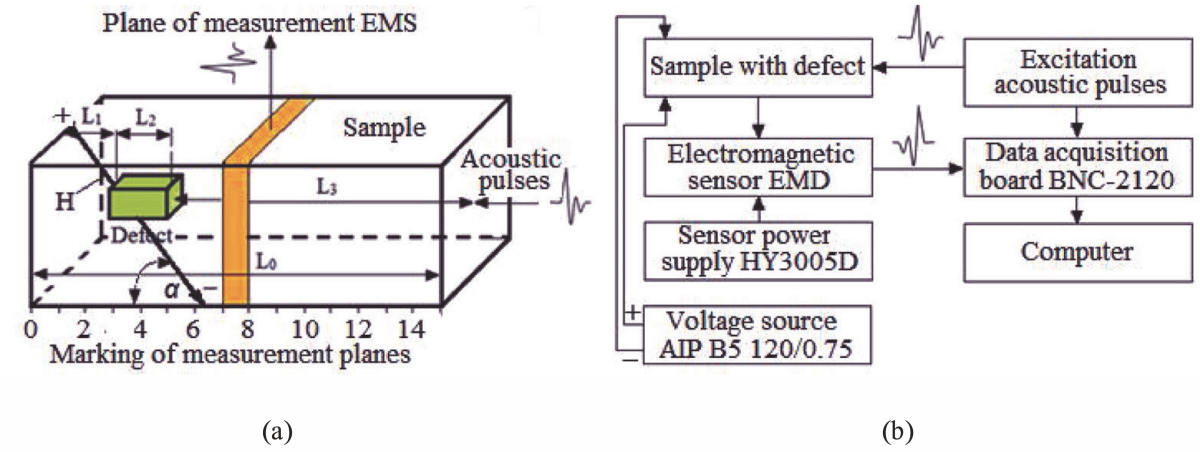

Figure 1. Model CSM samples with a defect inside exposed to pulsed acoustic excitation (a), and block diagram of the test bench to record and process excited electromagnetic pulses (b)

The changes in the parameters of the electromagnetic responses of the samples to acoustic exposure were experimentally studied using a special test bench. An acoustic pulse in the samples was excited by impact with a ball. The impact energy generated in the sample was determined by the time of the ball passage through two LED pairs. DC power supply AIP B5-120/0.75 was used as a voltage source to create an electric field. EMS was measured using an electromagnetic banded sensor along the length

of the sample with 15 measurement planes. At least 10 ball impacts and EMS measurements were performed on each plane. Figure 1*a* shows a model CSM sample with a defect in the form of an inclusion made of solid-state material, and figure 1*b* shows a block diagram of the test bench to record and process excited electromagnetic pulses.

The entire test bench was located inside a grounded electric shield to eliminate electromagnetic interference and reliably record EMS with amplitude of at least 2.0×10^{-3} V. A dynamic system of impact excitation with a ball ensured the duration of acoustic pulses of 5×10^{-5} at the base and of 3.5×10^{-5} seconds at a half width. The device that provides compression or extension of the spring was used to change the initial ball velocity. The time of the ball flight between two optical pairs, including LED and a photodetector was recorded to measure the velocity of the movement of the ball towards the sample and its rebound. This made it possible to generate the energy of the acoustic impact in the test sample in the range of $(8\div15)\times10^{-3}$ J. The dynamic system in the test bench can be replaced with a piezoelectric emitter with discretely adjustable duration of the exciting acoustic pulse ranging from 10^{-6} to 50×10^{-6} s. The same stand was used to measure the longitudinal speed of sound in test materials.

For experimental studies, a differential capacitive sensor (EMD), a differential amplifier, was used as a receiver of electromagnetic signals. The capacitive sensor consists of low-noise AD8627 (RC) microcircuits. At the sensor input, the remote controls were assembled as current feedback amplifiers to match high resistance of the receiving plates to the input resistance of the amplifier. In addition, the capacitive sensor was equipped with low and high frequency filters to ensure its operation in the range from 1 to 100 kHz. At the capacitive sensor output, the signal was amplified with a coefficient of 10 or 100. In measurements, the gain was chosen depending on the input EMS amplitude. The input EMD sensitivity was 2.0×10^{-4} V. The size of the receiving EMD plates in the experiments with CSM samples was $(0.5\times3.0)\times10^{-4}$ m^2. The distance from the surface of the test samples to the EMD plate was set equal to $(1–2)\times10^{-3}$ m. The signal from the electromagnetic sensor was transferred to the NI BNC-2120 data acquisition device and then to PC. Specially developed programs were used to normalize the EMS with regard to the vibrations induced by the ball impact, and its spectral analysis was performed using the fast Fourier transform (FFT) program to reveal its characteristic patterns for detecting solid-state defects.

3. Research result

To increase the EMS/noise ratio of the test bench, the effect of the applied electric field with variable intensity H on the parameters of the electromagnetic response under pulse acoustic exposure was studied first. Figure 1*b* shows the block diagram of the test bench. For this purpose, we changed the angle of incidence α of the electric field intensity vector to the contact surface of the cement-sand mixture and the front part of the defect (figure 1*a*), and the field strength was adjusted to H=2400 V/m. Figure 2*a* illustrates a regular increase in the EMS amplitude when the angle α increases. It should be noted that an increased angle of incidence and constant voltage across the electrodes decrease the H value from 2400 V/m to 1400 V/m due to the increased distance between the electrodes. The EMS amplitude attains its maximum when the location of the vector H is normal relative to the contact surface between the sample material and the defect in the form of a solid inclusion. Figure 2*b* shows the dependence of the EMS amplitude on the electric field strength at a constant angle of incidence α=45^o relative to the contact surface between the sample material and the fluoroplastic defect, and figure 3 presents similar dependence for the magnetite ore inclusion. The contact surfaces under study are perpendicular to the acoustic pulse propagation. As can be seen in figures 2*b* and 3, the EMS amplitude increases as the intensity of the electric field applied to the sample grows.

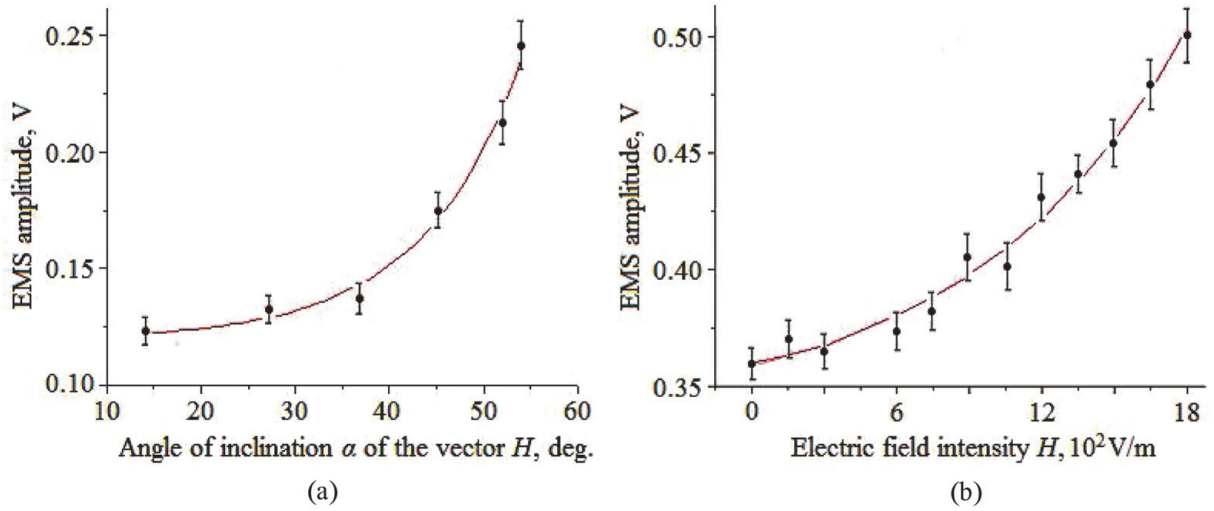

Figure 2. Changes in the amplitude of the electromagnetic signal depending on the angle of incidence α of the electric field strength vector H relative to the contact surface between the cement-sand mixture and the front part of the fluoroplastic defect with dimensions of $(10\times10\times15)\times10^{-9}$ m^3 (a) when the applied electric field increases and the angle α=45° is constant (b).

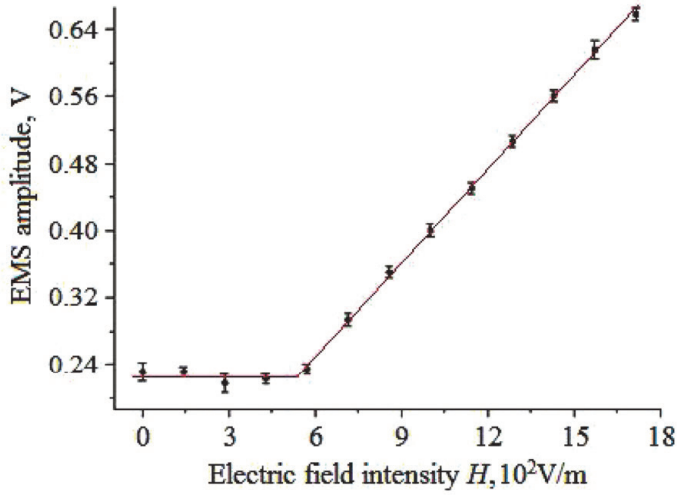

Figure 3. Changes in the amplitude of the electromagnetic signal at a constant angle α of the electric field intensity vector H relative to the contact surface between the cement-sand mixture and the front part of the magnetite ore defect with dimensions of $(10\times10\times15)\times10^{-9}$ m^3.

Thus, the experimental studies showed that the EMS amplitude increases when the angle of the electric field strength vector increases relative to the contact surface between the sample materials and defects. When the angle of incidence is constant, the EMS amplitude was found to increase when the field strength changed from zero to 18×10^2 V/m.

Figure 4 shows a sample with a fluoroplastic (PTFE) defect. The longitudinal speed of sound in PTFE is 1340 m/s at a density of ρ_{ptfe} = 2200 kg/m^3. The acoustic impedance of the cement-sand mixture in the sample is equal to z_{czm} = 5.25·106 kg/m^2·s, which is almost twice higher than that in PTFE, which corresponds to $z_{ptfe} = 2.95\cdot10^6$ kg/m^2·s. A defect with dimensions of $(10\times10\times15)\times10^{-9}$ m was at the level of measurement planes 3, 4, and partially 5. The acoustic pulse was injected from the side of measurement plane15.

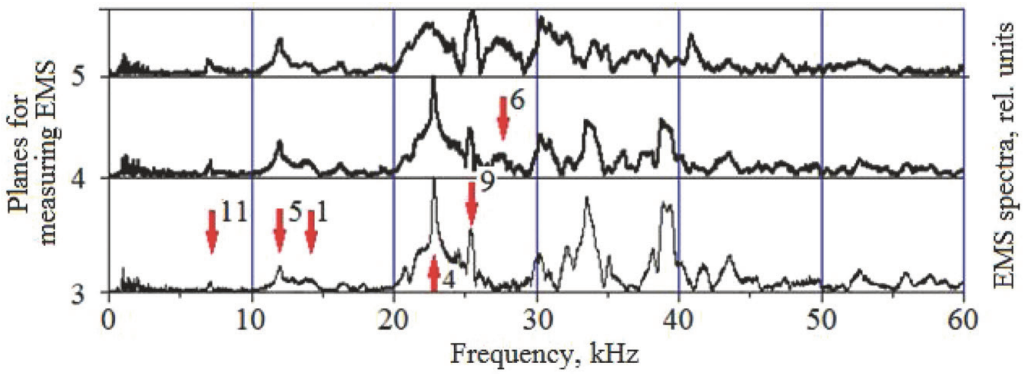

Figure 4. EMS spectra at different measurement planes of the model CSM sample with a fluoroplastic defect when excited by deterministic acoustic pulse.

Table 1 shows the calculation results for the EMS spectral components in the model CSM sample with a fluoroplastic inclusion when excited by determined acoustic pulse. The identity of the parameters of the acoustic pulses exciting the sample was monitored with regard to the velocity of the ball movement towards the surface. The frequencies were calculated using the formula $f_i = c_l/2L_i$, where f_i is the frequency component of the EMS spectrum; c_l is the longitudinal speed of sound in the basic material of the model sample or defect; L_i is the length of the sample part along which the acoustic pulse propagates. Figure 4 shows that measurement plane 3, which is at the farthest distance, exhibits the largest amplitude of the EMS spectral components. Other measurement planes are not presented here.

This indicates the presence of a defect in the sample volume. The propagation of the injected acoustic pulse along the sample length L_0 corresponds to the EMS spectral component of 14.55 kHz. In figure 4, this frequency is indicated by arrow 1. Other frequencies calculated and listed in the table also correspond to the EMS spectral components. The numbers indicating these frequencies correspond to those presented in Table 1. The frequencies indicated in figure 4 by arrows are crucial for identifying the defect location.

Table 1. The calculation results for the central spectral frequencies of electromagnetic signals in the CSM sample with a fluoroplastic inclusion under deterministic acoustic pulse excitation.

	Sample parts, 10^{-3} m	Double-pass time for the acoustic pulse, 10^{-6} s	Frequency of EMS spectrum, 10^3 Hz	Longitudinal speed of sound, c_l, m/s	Materials
1	$L_0 = 95$	68.70	**14.55**	2765	CSM
2	$L_1 = 20$	14.47	69.10	2765	CSM
3	$L_2 = 15$	22.39	44.67	1340	PTFE
4	$L_3 = 60$	43.47	**23.00**	2765	CSM
5	$L_0 + L_1$	83.30	**12.00**	2765	$CSM_{0,1}$
6	$L_1 + L_2$	36.86	**27.10**	2765_1, 1340_2	CSM_1, $PTFE_2$
7	$L_3 + L_2$	65.86	15.18	2765_3, 1340_2	CSM_3, $PTFE_2$
8	$L_1 + L_2 + L_3$	80.34	**12.45**	$2765_{1,3}$, 1340_2	$CSM_{1.3}$, $PTFE_2$
9	$L_0 + L_1 - L_3$	39.83	**25.11**	$2765_{0,1,3}$	$CSM_{0,1,3}$
10	$L_0 - L_3$	25.23	39.64	$2765_{0,3}$	$CSM_{0,3}$
11	$L_0 + L_1 + L_2 + L_3$	149.16	**6.7**	$2765_{0,1,3}$, 1340_2	$CSM_{0,1,3}$, $PTFE_2$

When the defect increases in size and the sample size remains constant, the spectrum changes and high-frequency spectral components of the EMS occur. Figure 5 shows the frequency spectra for fluoroplastic defects. In this case, the posterior boundary of the defect was at similar distance from the sample front, which was opposite to the acoustic pulse input upon the ball impact. Electromagnetic signals were recorded at measurement planes corresponding to the contact surface between the sample materials and defects located near the front part through which the acoustic pulse was injected.

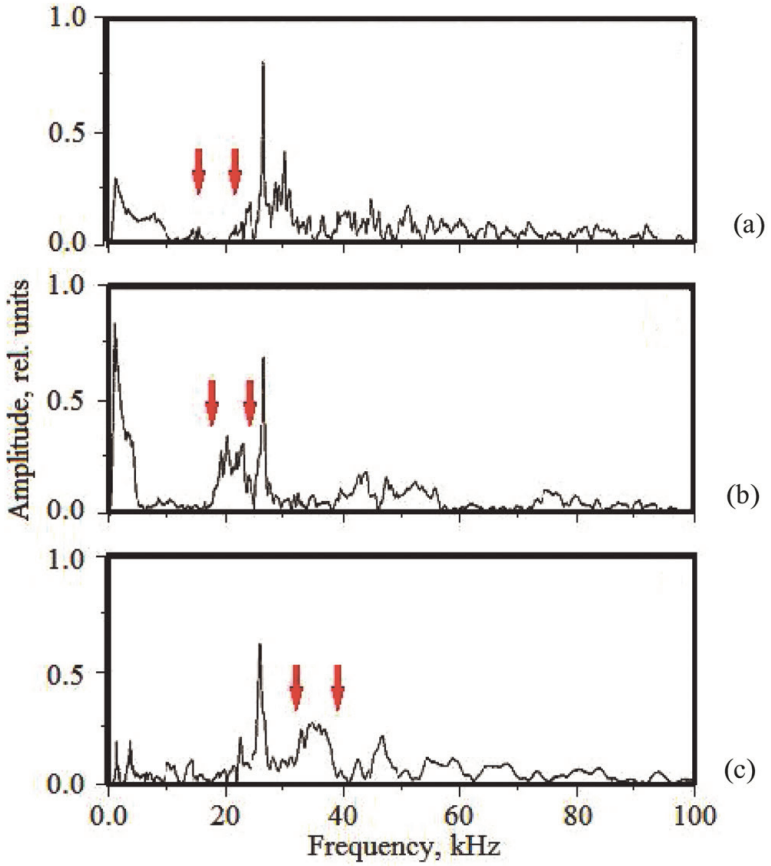

Figure 5. Changes in the spectrum of electromagnetic signals of the CSM sample with fluoroplastic defects of different sizes: (a) - $(10\times10\times15)\times10^{-9}$ m^3; (b) - $(20\times20\times30)\times10^{-9}$ m^3; (c) -$(25\times25\times38)\times10^{-9}$ m^3.

Frequency calculation showed that the largest spectral peak corresponds to the transverse sample size of 5.0×10^{-2} m. As noted above, the calculation of mechanical stresses at constant sample sizes and increased defect sizes shows a shift in the spectrum of acoustic vibrations to a higher frequency region due to the decreased distance between the walls of the sample and the defect. Since the parameters of the mechanical stresses observed during acoustic pulse propagation are directly related to electromagnetic responses, the EMS spectrum also changes [19]. In figure 5, arrows indicate changes in the spectrum corresponding to the defect length and the location of defects of different sizes.

4. Conclusion

Thus, the experimental studies showed that the EMS amplitude increases when the angle of the electric field strength vector increases relative to the contact surface of the sample materials and defects. Moreover, at a constant angle of incidence, the EMS amplitude increases as the field strength changes from zero to 18×10^2 V/m. This increase is due to the increased polarization of the contact

surface between the sample materials and defects in the form of solid inclusions. The applied electric field significantly improves the EMS/noise amplitude ratio.

The results of modeling showed the correspondence of the amplitudes of electromagnetic responses to the time and space distribution of mechanical stresses observed in the defective system during acoustic pulse propagation. It is shown that the parameters of electromagnetic signals indicate the distribution of the parameters of the exciting acoustic pulse in different parts of the sample volume, which is affected by the ratio of the acoustic impedance of the sample materials and defects. An increase in the defect size at constant sample size leads to changes in the spectrum and causes the occurrence of high-frequency spectral components of the EMS. In addition, the EMS spectra can be used to localize the dielectric defect in the dielectric material.

This study was supported by the Russian Science Foundation, grant 19-19-00178.

References

[1] *Physical Acoustics* (edited by W.P. Mason) 1964 **1** Part **A** (Academic Press New York) p 532
[2] Kluev V V 2008 *Nerazrushayushchiy kontrol'* [Non-destructive testing: Reference book in 8 volumes] (Moscow: Mashinostroenie)
[3] Blitz J 1997 *Electrical and Magnetic Methods of Non-destructive Testing* (Springer) p 261
[4] Ida N 1995 *Numerical Modeling for Electromagnetic Non-Destructive Evaluation* (Chapman & Hall edition, London) p 511
[5] Mikheev M N and Gorkunov E S 1993 *Magnitnyye metody strukturnogo analiza i nerazrushayushchego kontrolya* [Magnetic methods of structural analysis and non-destructive testing] (Moscow: Nauka) p 252
[6] Francesco Ficilli 2012 *Non-Destructive Testing by Magnetic Techniques* (LAP Lambert Academic Publishing) p 140
[7] Rumyantsev S V 1974 *Radiatsionnaya defektoskopiya* [Radiation flaw detection] (Moscow: Atomizdat) p 510
[8] *Nerazrushayushchiy kontrol'* [Nondestructive testing] (ed V V Sukhorukov) Book **4** 1992 (Moscow: Higher school) p 321
[9] Perelman M E, Khatiashvili N G 1981 O radioizluchenii pri khrupkom razrushenii dielektrikov [On radio emission during brittle destruction of dielectrics] *DAN SSSR* **256** (4) 824
[10] Rabinovitch A, Shay A, Liraz R, Frid V, Bahat D 2005 Electromagnetic radiation emitted during friction process *Int. J. of Fracture* **131**(2) 21
[11] Rabinovitch A, Frid V, Goldbaum J, Bahat D 2003 Polarization-depolarization process in glass during percussion drilling *Philosophical Magazine* **83**(25) 2929
[12] Frid V, Rabinovitch A, Bahat D 2003 Fracture induced electromagnetic radiation *J. of Physics D-Applied Physics* **36**(13) 1620
[13] Bespal'ko A A, Surzhikov A A, Yavorovich L V 2007 Study of Mechanoelectrical Transformation in Rocks Under Dynamic Impact *Russian Journal of Non-Ferrous Metals* **1** 9
[14] Miroshnichenko M I and Kuksenko V S 1980 Radiation of electromagnetic pulses during nucleation of cracks in solid dielectrics *Solid state physics* **22**(5) 1531
[15] O'Keefe S G and Thiel D V 1995 A mechanism for the production of electromagnetic radiation during fracture of brittle materials *Phys. Earth and Planet. Inter* **89**(11) 127
[16] Petrenko V F 1993 On the nature of electrical polarization of materials caused by cracks, application to ice *Philosophical Magazine B* **67**(3) 301
[17] Ogawa T, Oike K, Miura T 1985 Electromagnetic radiations from rocks *J. Geophys. Res.* **90** 6245
[18] Bespal'ko A A, Gol`d R M, Yavorovich L V and Datsko D I 2003 Excitation of electromagnetic radiation in laminated rocks under acoustic influence *Journal of Mining Science* **39**(2) 112

[19] Bespal'ko A A, Isaev Y N, Yavorovich L V 2016 Transformation of acoustic pulses into electromagnetic response in stratified and damaged structures *J.of Mining Sci.* **52**(2) 279
[20] Bespal'ko A A, Shtirts V A, Fedotov P I, Chulkov A O, Yavorovich L V 2019 Modelling of Infrared Glow in Rock Holes *Journal of Nondestructive Evaluation*) **38**(1) 31
[21] Fursa T V, Dann D D, Petrov M V, Lykov A E 2017 Evaluation of Damage in Concrete Under Uniaxial Compression by Measuring Electric Response to Mechanical Impact *J. of Nondestructive Evaluation* **36**(2) 30
[22] X-ray flat panel detector PerkinElmer XRD 0822 [*Electronic resource*]